Time Resolved MRA: Evaluation of Intrapulmonary Circulation Parameters in Pulmonary Arterial Hypertension

Hyun J. Jeong, PhD.[1], **Parmede Vakil, MS.**[1], **John J. Sheehan, MD.**[2], **Sanjiv J. Shah, MD.**[3], **Michael Cuttica, MD.**[4], **James C. Carr, MD.**[2], **Timothy J. Carroll, PhD.**[1,2], and **Amir Davarpanah, MD.**[2]

[1] Biomedical Engineering, Northwestern University

[2] Radiology, Northwestern University

[3] Cardiology, Northwestern University

[4] Pulmonary and Critical Care, Northwestern University

Abstract

Purpose—To determine whether pulmonary arterial and venous transit times measured by time-resolved MRA can be used as a diagnostic tool for pulmonary arterial hypertension (PAH).

Materials and Methods—12 patients with confirmed PAH and 10 healthy volunteers were scanned with IRB approval. Time-resolved MRA and 2D phase contrast flow images of the pulmonary vasculature were acquired. Pulmonary arterial and venous transit times (PaTT and PvTT) and pulmonary valve flow (PVF) were obtained. Pulmonary arterial and pulmonary venous blood volumes (PaBV and PvBV) were calculated as the product of flow and transit time.

Results—Patients with PAH showed statistically significant increases in PaTT and PvTT ($p<0.0004$, $p<0.05$ respectively) compared to controls. PaBV (165.2 ± 92.0ml) was significantly higher in PAH subjects than controls (97.0 ± 47.1 ml) ($p<0.04$), whereas PvBV (127.9 ± 148.9ml) of PAH subjects had no significant increase from those of healthy controls (142.5 ± 104.1 ml) ($p<0.38$).

Conclusion—Pulmonary arterial transit times measured using time-resolved MRA can be used as a simple, non-invasive metric for detection of altered hemodynamics in PAH.

Keywords

pulmonary hypertension; angiography; time-resolved; contrast-enhanced

INTRODUCTION

Pulmonary arterial hypertension (PAH) is a disease of the pulmonary arteries that is characterized by vascular proliferation and remodeling (1–2). It results in restricted flow through the pulmonary arterial circulation with a progressive increase in pulmonary vascular resistance and ultimately right ventricular failure and death. The imbalance in the vasoconstrictor/vasodilator milieu has served as the basis for current medical therapies, although increasingly it is recognized that PAH also involves an imbalance of proliferation and apoptosis. There are a large number of causes for PAH, and they can be broadly divided

Corresponding author: Timothy J. Carroll, PhD, 737 North Michigan Avenue, Suite 1600, Chicago, IL 60611, Phone: 312-926-1733, Fax: 312 926 5991, t-carroll@northwestern.edu.

into primary (idiopathic) and secondary causes. The current diagnostic classification of PAH was established during the 2008 World Symposium on Pulmonary Hypertension (3).

Diagnosis of PAH is based on right heart catheterization (RHC) and is defined by a mean pulmonary artery pressure (mPAP) ≥ 25 mmHg at rest in the setting of a normal or reduced cardiac output (CO) and a normal pulmonary capillary wedge pressure (4). RHC, however, is an invasive test with a small but well-defined morbidity and mortality. Therefore, the availability of a non-invasive surrogate for evaluating PAH would be highly desirable.

Contrast-enhanced MR angiography (CEMRA) has been used successfully to evaluate the pulmonary arterial system for indications such as pulmonary thromboembolic disease and congenital heart disease (5–7). However, conventional CEMRA has long acquisition times when compared to the typical pulmonary arteriovenous transit time leading to venous signal overlaying arteries, which may potentially obscure pathology. Additionally, conventional CEMRA produces no dynamic information about the pulmonary circulation. Time-resolved MRA (TRMRA) has been shown to produce dynamic information in the pulmonary circulation(8–9) and has been utilized for depicting both vascular pathology and measuring pulmonary transit times (5,9–10). Currently utilized TRMRA techniques can demonstrate large differences in transit between the pulmonary trunk and aorta but lack the dynamic information to show differences between different portions of the pulmonary circulation. Other high frame rate TRMRA techniques have improved temporal resolution but have sacrificed SNR (SENSE and CENTRA-Keyhole) (9) or spatial resolution (10), which could compromise anatomical depiction. A TRMRA technique which maintains adequate spatial resolution to visualize small branch vessels and temporal resolution to demonstrate small differences in transit between the pulmonary arteries and veins may be a strong clinical tool in the setting of pulmonary hypertension.

The purpose of our study was to test the hypothesis that pulmonary arterial and venous blood volumes and transit times measured by a new high frame rate, time-resolved MRA sequence effect the physiological changes resulting from PAH.

MATERIALS AND METHODS

With IRB approval, we conducted a retrospective review of 12 patients (1 male, 11 female, mean age 51.9 ± 14.5, range 30–79 years, weight 71.5 +/− 20.4 kg) with RHC-confirmed, PAH (mPAP > 25 mmHg, range 26–60 mmHg) who underwent TRMRA within 13 months of their RHC exam. All 12 patients were among Group I type pulmonary arterial hypertension (PAH) (3). Left-sided causes were ruled out based on right and left heart catheterization. The patient group consisted of one subject with idiopathic PAH (IPAH) and 11 subjects with PAH secondary to collagen vascular diseases (8 systemic sclerosis, 2 mixed connective tissue disease, 1 systemic lupus erythematosus). Six patients were identified to have RV dysfunction based on RV ejection fraction <35% (11). The control group consisted of 10 healthy (asymptomatic) volunteers (3 male, 7 female, mean age 32.7±11.8, range 25–65 years, weight 64.3 +/− 26.8 kg), recruited with IRB approval and informed consent, to undergo an identical TRMRA protocol. All studies were carried out on a 1.5T scanner (21 on Avanto, 1 on Espree; Siemens Medical Systems, Erlangen, Germany) using a phased array body coil for signal reception.

Time- Resolved MRA

All MRA images were acquired using a time-resolved MRA technique that was proven useful in intracranial MRA applications (12–15). The technique is based on 3D radial ("stack of stars") *k*-space with sliding window reconstruction (16) and sliding mask subtraction (12). Sliding window reconstruction produces intermediate images between

measurements to increase the apparent frame rate of time-resolved MRA, and it is well suited for radial *k*-space in particular since the center of *k*-space is acquired in each radial projection (Figure 1a, b). Sliding mask-mode subtraction in which the subtraction mask follows a fixed time interval behind the reconstructed frame improves the separation of signal from arteries and veins. This is advantageous when trying to distinguish the distal branches of arteries from veins for accurate transit time measurements.

Figure 1c illustrates the acquisition scheme for time-resolved MRA. The scan protocol includes a set of three consecutive scans with breath holds. For the first scan, the first pre-contrast mask, one measurement (a complete set of 3D *k*-space lines) was acquired with a breath hold, which lasts roughly 15 seconds. After a 15-second break and normal breathing, another measurement was acquired with breath hold. After another 15 second break, 6mL of contrast agent (Magnevist, Berlex, Wayne, NJ; Multihance, Bracco, Princeton, NJ) is injected at 4mL/s, and 4 measurements are acquired, lasting about a minute, while the subject holds his breath for as long as possible. Magnevist was the primary contrast agent utilized except for subjects with low-GFR, in which case, Multihance was used as stipulated by our institution's clinical protocol as well as IRB mandates.

Patient images were acquired in the LAO projection in accordance with our institutions cardiopulmonary, TRMRA dose-timing run protocol. Healthy volunteers were scanned using the same view to maintain continuity. Each TRMRA acquisition utilized the same sequence parameters as listed: Number of projection (N_P) =192, readout points (N_{RO}=192, 75% fractional echo), FOV=280mm × 280mm, slices = 30 (23 acquired with 75% partial Fourier), slice thickness = 3.0 mm, pixel size = 1.5 × 1.5 × 3.0 mm, Tip angle =30°, TR/TE=2.8/1.4 ms. Sixteen intermediate images were reconstructed with sliding window reconstruction, resulting in a frame rate of approximately 0.7 second/frame.

Phase contrast flow quantification

Through-plane 2D phase contrast flow quantification was performed perpendicular to the main pulmonary artery (PVF) with the following parameters: TR=49 ms, TE=3.1 ms, flip angle=25°, cardiac phases 20, sequence acquisition time = ~13 s, bandwidth 355.0 Hz/pixel, FOV= 244×340 mm, matrix size 103×192 mm, pixel size=2.3×1.7 mm, slice thickness=6.0 mm. A velocity limit of 100 cm/sec was used and it was increased if aliasing was observed.

Image Analysis

Intrapulmonary transit times (PaTT = Pulmonary arterial transit time, PvTT = Pulmonary venous transit time) were determined from subtracted maximum intensity projections from the time resolved MRA images from the LAO projection using an offline workstation (Leonardo, Siemens Medical Solutions, Malvern, PA, USA). For transit time calculations ROIs were placed to cover the proximal and distal pulmonary arteries and proximal and distal pulmonary veins, for the determination of arterial and venous transit times, respectively (Figure 2). The time difference between peak signal enhancements at two ROIs served as a measure of the bolus transit time through the pulmonary arteries and veins (Figure 2). In order to standardize the effect of image quality on the visualization of the most distal arterial segment, ROIs were placed on the distal left pulmonary artery at the level of the right ventricle apex. PaTT was calculated as time between peaks at ROIs 1 and 2. PvTT was calculated as time between peaks at ROIs 3 and 4.

Pulmonary arterial blood volume (PaBV) and pulmonary venous blood volume (PvBV) was calculated by multiplying the average blood flow (PC flow imaging) through the pulmonary valve (PVF, mL/s) by the bolus transit time from the proximal to the distal pulmonary artery and from the proximal to the distal pulmonary vein respectively (TRMRA) (17).

Statistical Analysis

Statistical analyses were performed using commercially available software (SPSS, version 13.0; SPSS, Chicago, Ill). Transit times and ventricular volumetric values for the PAH group were compared with those for the control subjects by using two-tailed Students t-tests. Sensitivity and specificity for detecting PAH were calculated for various transit time cutoffs. To determine the ability of MR-derived parameters to depict the presence of PH, receiver operating characteristic (ROC) curve analysis was performed, and sensitivity and specificity were calculated. However, due to the small sample size, confidence interval coverage allowed only relative comparisons of areas under the curve (AUCs) for different MR-derived parameters (18). A p-value of less than 0.05 was considered to indicate a significant difference in all tests.

RESULTS

All examinations were successful and there were no adverse events reported. Figure 3a shows representative maximum intensity project (MIP) images reconstructed at 714 ms time intervals. Clear depiction of the distal pulmonary branches is demonstrated in Figure 3b which shows conventional mask mode subtraction and the sliding mask. The sliding mask subtracts out the trailing edge of the bolus, suppressing arterial signal in the venous phase.

In assessing PAH, LV disease was excluded from both patients and controls due to physiologically normal cardiac output in both groups. Furthermore, differences in CO between patient and control groups were found to be statistically insignificant (*p=0.44*). A comparison between arterial and venous transit times and blood volumes, as well as pulmonary valve flow rates are reported in Table 1. We found statistically significant (*p<0.05*) prolongation between the transit time compared to controls. The degree to which the transit time was lengthened was greater for the arteries, PaTT, (1.92 times) when compared to the veins, PvTT (1.4 times greater). This observation is consistent with the differential diagnosis of arterial and venous hypertension. Statistically greater PaBV values were also seen in PAH patients (*p<0.04*).

Only PaTT and total transit time (TT = PaTT + PvTT) had a statistically significant areas under the curve (AUC) (Figure 4). PaTT and TT had AUC values of 0.938 (*p=0.001*) and 0.925 (*p=0.001*) respectively, while PvBV and PaBV had AUC values of 0.467(p=*0.792*) and 0.733 (p=*0.065*), respectively. For a cutoff value of 2 seconds PaTT had a sensitivity of 92% and specificity of 90% for detection of PAH. The cutoff value of 2.25 seconds resulted in a sensitivity of 83% and a specificity of 100%.

DISCUSSION

Our radial sliding window time-resolved MRA technique provides high frame rate depiction of pulmonary hemodynamics allowing successful calculation of transit times within the pulmonary circulation, which can be used to detect pulmonary arterial hypertension. Furthermore, the use of sliding mask subtraction provides greater separation of arterial and venous signal improving the accuracy of our calculations. Ultimately, TRMRA may prove to be a strong non-invasive adjunct to right heart catheterization in the diagnosis and therapy of PAH patients.

PaTT, as measured by radial sliding window TRMRA, were significantly prolonged in patients with PAH. PvTT values were also prolonged, but this had less significance. The greater prolongation of PaTT may be indicative of arterial pathology in a PAH group; however further study is required in separate PAH and PVH settings for further validation. ROC curves showed PaTT in particular had a higher sensitivity and specificity for detecting

PAH than other parameters. This may be a useful method for diagnosis of PAH patients; however a larger sample size is necessary for a more conclusive ROC analysis of PaTT sensitivity to PAH. PaBV was also increased in PAH patients; however it was not as sensitive to detecting PAH as PaTT or TT. It has been suggested that an increase in pulmonary blood volume is the main reason for vascular remodeling and resultant pulmonary hypertension during chronic hypoxia (19). Such increases have also been found to be correlated with measures of RV dysfunction such as lower ejection fraction and ventricular dilation (17). The result of our study shows the arterial blood volume in patients with PAH is significantly higher than controls. This might suggest the main pathophysiology of PAH and can be further used to follow up treatment in this group.

There was a moderate linear correlation between PaTT and mPAP (r = 0.3), PvTT and mPAP (r = 0.2), PaTT and PVR (r = 0.4), and PvTT and PVR (r = 0.5), making nonlinear relationships more likely, which is to be expected. However, further interpretation of these results is limited as the patient recruitment criteria eliminated subjects with low mPAP, and mPAP and PVR values could not be gathered for controls due to the invasive nature of the procedure. Without a full range of mPAP values, the full strength of this correlation cannot be determined. Therefore, we must rely on the results of a paired two sample t-test, which determined a significant difference between PvTT and PaTT among PAH cases and controls. These suggest PaTT and PvTT may be used as a diagnostic tool in the setting of PAH.

In fact, prolonged PaTT may be a direct indicator of elevated pressure in the pulmonary arterial system and right heart failure. The results are consistent with what Shors et al. reported on the left heart where transit times were used to predict left heart failure. They showed prolongation of transit times in patients with left ventricle (LV) dysfunction and their direct correlation with LV volumes and inverse correlation with LV ejection fraction (EF) (5). It has been shown that patients with a history of LV diseases showed prolonged arm-to-aorta transit times (20). In our study however, the patients were confirmed with normal physiological parameters. Therefore, left ventricular conditions can be excluded as causes of prolonged transit times in the pulmonary arteries.

With previous TRMRA studies, it was necessary to significantly trade off spatial resolution (8) (10) or SNR (9) to achieve near-subsecond temporal resolution, thus compromising depiction of vascular anatomy. However, with the radial sliding window MRA, it is possible to measure transit times between different parts of the pulmonary circulation while preserving adequate spatial resolution for a truer representation of pulmonary vasculature and hemodynamics. This, in addition to the transit times and total blood volume measurements, could be a useful parameter for determination of pulmonary hypertension.

Time-resolved MRA has not been yet used often as a quantification tool, mainly due to the fact that the fidelity of the dynamic information is affected by the temporal footprint, the length of the time to acquire a single frame, and the *k*-space acquisition scheme (21). Sliding window reconstruction uses view sharing to increase the frame rate, but not necessarily the temporal resolution, since the temporal footprint is unchanged. It has been shown that a long temporal footprint blurs the temporal profile of the dynamic MRA (15,22–23). Therefore, full-width at half maximum of the contrast curves which is sometimes used to quantify functional parameters (5) must be carefully used, since it is strongly dependent on the MR sequence parameters such as *k*-space ordering scheme and acquisition durations. For this study, transit times were obtained by measuring the time between the peak contrast signals, which should be independent of the temporal footprint.

A subject undergoes 3 separate breath holds during the 4D MRA scan, and misregistrations of the post-contrast images and the pre-contrast images are possible. This has not been a problem in our scans. The position of the chest during each breath hold has been consistent. In addition, sliding mask subtraction is less susceptible to this problem since the mask is continuously updated. The purpose of the first set is for the initial subtraction mask, and the purpose of the second set is to provide a contrast-free phase so that the very beginning of the contrast passage can be captured. The use of the multiple breath hold protocol also has improved the length and stability of the breath hold used for the contrast injection. The injection needs to occur after two measurements to provide enough pre-contrast data after the subtraction mask since the transit time from antecubital vein to the heart is relatively short compared to the head or the extremities.

There were some limitations in this study due mainly to its retrospective nature. As a result, some variables could not be controlled. SNR may have varied for cases where a different MRI scanner was utilized or different contrast agent was applied; however, the temporal resolution and dynamic information remained unaffected as identical pulse sequence protocols were used. Only patients with confirmed PAH were studied. Therefore, it is not yet known how the measured parameters differ in patients with pulmonary venous hypertension. PAH could not be excluded in volunteers due to the invasive nature of RHC; however due to the low prevalence of PH in the young population(< 35 years) and a young control group (mean age 32 years) consisting of asymptomatic individuals with no cardiopulmonary disease risk factors(normal CO and EF), the existence of undiagnosed PH is unlikely (24).

Patients and controls were not age matched; however mPAP at rest has been shown to be "virtually independent of age," therefore no significant bias is expected (25). Furthermore, heart rate can be excluded as a confounding factor as studies have shown no correlation with contrast bolus kinetics in CEMRA (26) unless in the case of compromised cardiac output (20). No conclusions can be drawn on the reproducibility of TT determination by TRMRA since measurements were only taken once for each subject; however derived values in our control group closely correspond to published literature (5).

In conclusion, pulmonary arterial transit times measured using time-resolved MRA can be used as a simple, non-invasive metric for detection of altered hemodynamics in PAH. If validated in future studies, time-resolved MRA may offer an important non-invasive adjunct to RHC for the diagnosis of patients with PAH.

Acknowledgments

References

1. Galie N, Hoeper MM, Humbert M, et al. Guidelines for the diagnosis and treatment of pulmonary hypertension: The Task Force for the Diagnosis and Treatment of Pulmonary Hypertension of the European Society of Cardiology (ESC) and the European Respiratory Society (ERS), endorsed by

the International Society of Heart and Lung Transplantation (ISHLT). Eur Heart J. 2009; 30(20): 2493–2537. [PubMed: 19713419]

2. McLaughlin VV, Archer SL, Badesch DB, et al. ACCF/AHA 2009 expert consensus document on pulmonary hypertension: a report of the American College of Cardiology Foundation Task Force on Expert Consensus Documents and the American Heart Association: developed in collaboration with the American College of Chest Physicians, American Thoracic Society, Inc. and the Pulmonary Hypertension Association. Circulation. 2009; 119(16):2250–2294. [PubMed: 19332472]

3. Simonneau G, Robbins IM, Beghetti M, et al. Updated clinical classification of pulmonary hypertension. J Am Coll Cardiol. 2009; 54(1 Suppl):S43–54. [PubMed: 19555858]

4. Barst RJ, McGoon M, Torbicki A, et al. Diagnosis and differential assessment of pulmonary arterial hypertension. J Am Coll Cardiol. 2004; 43(12 Suppl S):40S–47S. [PubMed: 15194177]

5. Shors SM, Cotts WG, Pavlovic-Surjancev B, Francois CJ, Gheorghiade M, Finn JP. Heart failure: evaluation of cardiopulmonary transit times with time-resolved MR angiography. Radiology. 2003; 229(3):743–748. [PubMed: 14657311]

6. Kellenberger E, Springael JY, Parmentier M, Hachet-Haas M, Galzi JL, Rognan D. Identification of nonpeptide CCR5 receptor agonists by structure-based virtual screening. J Med Chem. 2007; 50(6): 1294–1303. [PubMed: 17311371]

7. Ley S, Kauczor HU. MR imaging/magnetic resonance angiography of the pulmonary arteries and pulmonary thromboembolic disease. Magn Reson Imaging Clin N Am. 2008; 16(2):263–273. ix. [PubMed: 18474331]

8. Carr JC, Laub G, Zheng J, Pereles FS, Finn JP. Time-resolved three-dimensional pulmonary MR angiography and perfusion imaging with ultrashort repetition time. Acad Radiol. 2002; 9(12):1407–1418. [PubMed: 12553352]

9. Korperich H, Gieseke J, Esdorn H, et al. Ultrafast time-resolved contrast-enhanced 3D pulmonary venous cardiovascular magnetic resonance angiography using SENSE combined with CENTRA-keyhole. J Cardiovasc Magn Reson. 2007; 9(1):77–87. [PubMed: 17178684]

10. Ley S, Fink C, Zaporozhan J, et al. Value of high spatial and high temporal resolution magnetic resonance angiography for differentiation between idiopathic and thromboembolic pulmonary hypertension: initial results. Eur Radiol. 2005; 15(11):2256–2263. [PubMed: 16041529]

11. La Vecchia L, Zanolla L, Varotto L, et al. Reduced right ventricular ejection fraction as a marker for idiopathic dilated cardiomyopathy compared with ischemic left ventricular dysfunction. Am Heart J. 2001; 142(1):181–189. [PubMed: 11431676]

12. Cashen TA, Jeong H, Shah MK, et al. 4D radial contrast-enhanced MR angiography with sliding subtraction. Magn Reson Med. 2007; 58(5):962–972. [PubMed: 17969099]

13. Eddleman CS, Jeong H, Cashen TA, et al. Advanced noninvasive imaging of spinal vascular malformations. Neurosurg Focus. 2009; 26(1):E9. [PubMed: 19119895]

14. Eddleman CS, Jeong HJ, Hurley MC, et al. 4D radial acquisition contrast-enhanced MR angiography and intracranial arteriovenous malformations: quickly approaching digital subtraction angiography. Stroke. 2009; 40(8):2749–2753. [PubMed: 19478223]

15. Jeong HJ, Cashen TA, Hurley MC, et al. Radial sliding-window magnetic resonance angiography (MRA) with highly-constrained projection reconstruction (HYPR). Magn Reson Med. 2009; 61(5):1103–1113. [PubMed: 19230015]

16. Riederer SJ, Tasciyan T, Farzaneh F, Lee JN, Wright RC, Herfkens RJ. MR fluoroscopy: technical feasibility. Magn Reson Med. 1988; 8(1):1–15. [PubMed: 3173063]

17. Lakoma A, Tuite D, Sheehan J, Weale P, Carr JC. Measurement of pulmonary circulation parameters using time-resolved MR angiography in patients after Ross procedure. AJR Am J Roentgenol. 2010; 194(4):912–919. [PubMed: 20308491]

18. Obuchowski NA, Lieber ML. Confidence intervals for the receiver operating characteristic area in studies with small samples. Acad Radiol. 1998; 5(8):561–571. [PubMed: 9702267]

19. Ou LC, Sardella GL, Hill NS, Thron CD. Possible role of pulmonary blood volume in chronic hypoxic pulmonary hypertension. J Appl Physiol. 1993; 74(6):3020–3026. [PubMed: 8366002]

20. Francois CJ, Shors SM, Bonow RO, Finn JP. Analysis of cardiopulmonary transit times at contrast material-enhanced MR imaging in patients with heart disease. Radiology. 2003; 227(2):447–452. [PubMed: 12676971]

21. Mostardi PM, Haider CR, Rossman PJ, Borisch EA, Riederer SJ. Controlled experimental study depicting moving objects in view-shared time-resolved 3D MRA. Magn Reson Med. 2009; 62(1): 85–95. [PubMed: 19319897]

22. Huang Y, Wright GA. Time-Resolved MR Angiography with Limited Projections. Proc Intl Soc Magn Reson Med. 2007; 15:181.

23. Jeong H, Shah S, Eddleman CS, Sheehan JJ, Carr JC, Carroll TJ. Time-Resolved MRA uUsing Radial Mulit-Echo Sequence and Sliding Window Reconstruction. Proc Intl Soc Magn Reson Med. 2009; 17:4723.

24. Rich S, Chomka E, Hasara L, et al. The prevalence of pulmonary hypertension in the United States. Adult population estimates obtained from measurements of chest roentgenograms from the NHANES II Survey. Chest. 1989; 96(2):236–241. [PubMed: 2787729]

25. Kovacs G, Berghold A, Scheidl S, Olschewski H. Pulmonary arterial pressure during rest and exercise in healthy subjects: a systematic review. Eur Respir J. 2009; 34(4):888–894. [PubMed: 19324955]

26. Hany TF, McKinnon GC, Leung DA, Pfammatter T, Debatin JF. Optimization of contrast timing for breath-hold three-dimensional MR angiography. J Magn Reson Imaging. 1997; 7(3):551–556. [PubMed: 9170041]
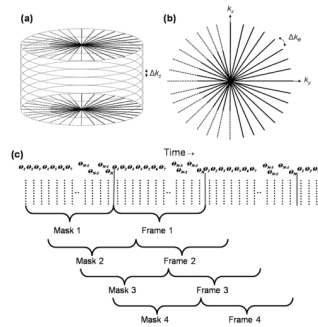
Figure 1.
(a) The Time resolved MRA pulse sequence employs a radial "stack of stars" acquisition scheme, with radial in-plane and Cartesian through-plane sampling. All slice encodings are looped inside each projection angle. (b) Radial in-plane k-space sampling with partial echo. (c) Intermediate image from each 3D volume are reconstructed using a sliding window view-sharing and sliding subtraction mask scheme to provide improved separation of the signal form arteries and veins.
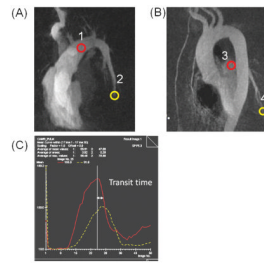
Figure 2. MRA signal curves were obtained by placing ROIs on proximal artery (1), distal artery (2), proximal vein (3), and distal vein (4)
Transit times were determined by measuring the time between the peaks of proximal and distal ROIs
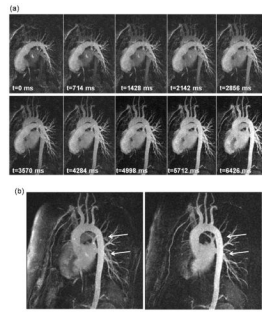
Figure 3. A representative time resolved MRA exam
(a) Consecutive intermediate time frames reconstructed at 714 ms time intervals are shown.
(b) Comparison of conventional (left) and sliding (right) subtraction mask. The subtraction mask suppresses arterial signal (arrows) for better depiction of pulmonary veins.
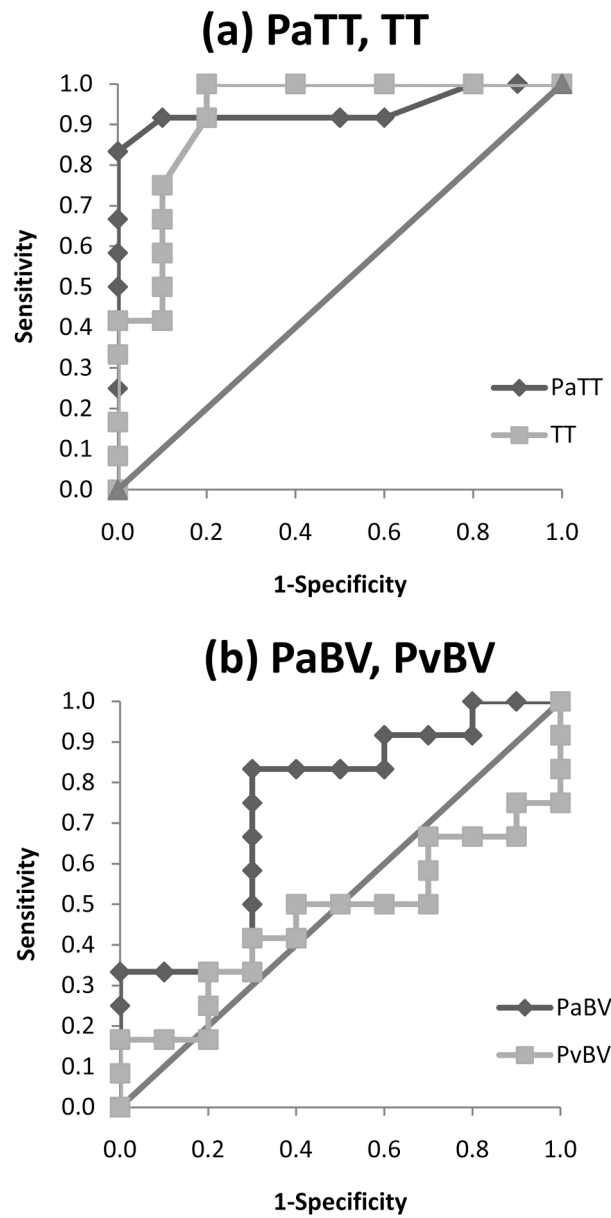
(a) PaTT, TT

(b) PaBV, PvBV

Figure 4. (a) ROC curve for PaTT and TT; (b) ROC curve for PaBV, and PvBV
Transit time is a better indicator of PAH than blood volume. PaTT and TT had statistically significant AUC.

Table 1

Average Arterial and Venous Transit Times, Blood Volumes, and Flow Rates for PAH Patients and control subjects

	Transit Time (s)		Blood Volumes (ml)		Flow (ml/s)
	Arterial	**Venous**	**Arterial**	**Venous**	**PVF**
PAH	**2.7 ± 1.0**	2.2 ± 0.9	165 ± 92.0	152 ± 133	61.6 ± 39.2
Controls	**1.4 ± 0.5**	1.6 ± 0.6	95.0 ± 47.1	117 ± 62.0	70.2 ± 19.2
P-value	*<0.0004*	*<0.05*	*<0.04*	*0.54*	*0.27*

PAH = Pulmonary Arterial Hypertension

PVF=Pulmonary Valve Flow

MVF=Mitral Valve Flow